

# MICROFABRICATION OF ELECTROCHEMICAL CAPACITORS WITH VERTICALLY-ALIGNED CARBON NANOTUBE ELECTRODES

Hyun Jin In, Betar Gallant, Yang Shao-Horn, and George Barbastathis

Department of Mechanical Engineering, Massachusetts Institute of Technology, USA

**Abstract:** Densely packed arrays of vertically-aligned carbon nanotubes (CNTs) make ideal electrodes in electrochemical capacitor applications due mainly to the CNTs' high surface area and electrical conductivity. In this paper, we present an origami-based microfabrication process for creating microscale supercapacitors with CNT electrodes that are grown directly on the device. The completed device was subjected to electrochemical analysis and found to exhibit a relatively high capacitance of  $0.4 \mu\text{F}$  from an electrode area measuring only  $250 \mu\text{m} \times 250 \mu\text{m}$ . The CNT-origami supercapacitor holds promise as an efficient on-chip power source for numerous autonomous MEMS-based system applications.

**Keywords:** electrochemical capacitor, supercapacitor, carbon nanotubes, MEMS

## INTRODUCTION

An electrochemical capacitor, also commonly known as a supercapacitor, is a type of capacitor in which the energy is stored within an electrochemical double layer at the electrode/electrolyte interface [1]. Such devices derive their high capacitance mainly from the large surface area of the extremely porous electrode material. Various forms of carbon, including carbon nanotubes (CNTs), make excellent supercapacitor electrodes largely because of their high conductivity and specific surface area [2,3], and they are commonly used in macroscale devices for many research and commercial applications.

In our previous work [4], microfabricated electrochemical capacitors were made by integrating the Nanostructured Origami™ process with a manual carbon-electrode deposition step; the origami process consists of first patterning a two-dimensional (2-D) membrane with micro/nano-scale features and then folding the membrane into the desired three-dimensional (3-D) configuration as will be described in the next section. The origami process, which enabled the integration of nanoscale features and 3-D architecture, proved ideal for electrochemical capacitor microfabrication, and the nanostructured electrodes resulted in a  $50\times$  increase in capacitance compared to devices without such electrodes [4].

In this paper, we report on the origami-based fabrication and testing of a microfabricated electrochemical capacitor with nanostructured electrodes consisting of *in-situ* grown, vertically-aligned multiwalled carbon nanotubes (MWCNTs) as seen in Fig. 1. The device consists of a single CNT electrode flap that flips over to create the top/bottom electrode architecture. The process reported herein remains compatible with many MEMS-based processes, thus ensuring integration with pre-existing

micro/nano-systems for possible use as an on-chip power source. As is the case with macroscale supercapacitors based on CNT electrodes, the densely packed arrays of vertically-aligned MWCNTs in the CNT-origami supercapacitor are expected to provide excellent electrical conductivity, high surface area, and superior electrolyte accessibility due to the presence of larger pores and conductive paths [5,6]. While macroscale electrochemical capacitors based on CNT electrodes have been demonstrated previously [7], the direct growth of the CNTs on the current collector, as opposed to the post-growth transfer of CNTs, will help minimize contact resistance between the CNTs and the substrate while eliminating CNT-to-CNT resistance within the electrode network.

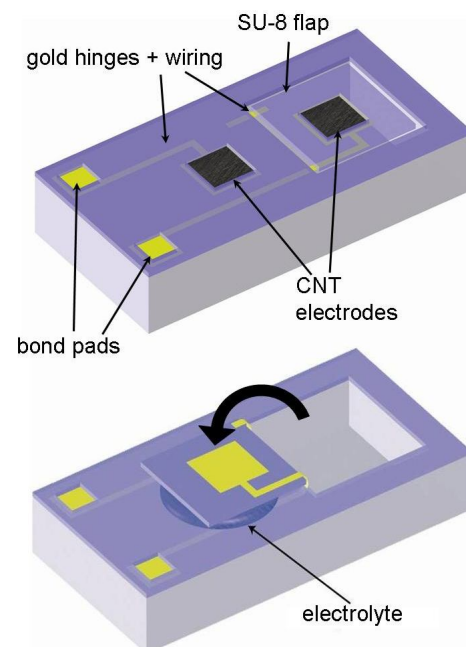


Fig. 1: Schematic of the CNT-origami supercapacitor before and after the folding process.

## FABRICATION

The fabrication process for the CNT-origami supercapacitors is based closely on our previously reported origami process [4]. However, the direct growth of CNTs requires exposure to temperature as high as 700°C. The high temperature may damage the current collectors if they are made out of gold, as is customary. Therefore, our CNT-origami process begins by first depositing and patterning two, 150 nm thick titanium nitride (TiN) current collectors that will later form the opposing electrodes of the supercapacitor (Fig. 2a). At this stage, a thin layer (~20 nm) of nickel (Ni) is deposited on top of the TiN sections to serve as catalysts for CNT growth (Fig. 2b). The TiN layer should provide good electrical connectivity to the nanotubes while serving as an excellent diffusion barrier layer and also enhancing nanotube growth [8]. A densely packed array of vertically-aligned MWCNTs is then grown out of the catalyst layer following up to 30 minutes of growth in a 4:1 flow of ammonia and acetylene gases under a 150W DC plasma (Fig. 2c). Variations in catalyst thickness and in the growth process yield nanotubes of different diameters, densities, and lengths. A typical CNT array used in our experiments had a density of  $\sim 9$  CNTs/ $\mu\text{m}^2$  with individual CNT diameter and length of approximately 150 nm and 5  $\mu\text{m}$ , respectively. A 20 nm thick layer of silicon nitride (SiN) that covers the entire substrate (not shown in the drawing) provides electrical isolation between the device and the silicon substrate. In addition to the use of TiN, direct growth of CNTs on a metallic alloy substrate [9] as well as a Mo/Al/Fe metal stack [10] have been recently demonstrated by other groups.

The remainder of the origami fabrication process takes place after the CNTs have been grown. In Fig. 2d, a 600 nm thick gold layer is deposited using the photoresist lift-off technique to create the necessary hinge and wiring elements. As shown in the inset in Fig. 3, the CNTs remained resilient to standard lift-off processing with the only caveat being that the thickness of the photoresist layer used for lift-off must be sufficiently thick to conformally cover the tips of the CNTs. In Fig. 2e, a SU-8 layer is deposited and photolithographically patterned around the electrodes to provide overall structural support during and after the folding process. The SU-8 layer is typically  $\sim 10$   $\mu\text{m}$  thick but the thickness can be adjusted to account for different CNT heights. In the final step of the fabrication process (Fig. 2f), the folding segment is released from the substrate through a  $\text{XeF}_2$  isotropic dry etching of the underlying silicon. Folding is

accomplished by applying a small drop of electrolyte (1M  $\text{H}_2\text{SO}_4$ ) to the device, at which point the loose flap flips over due to capillary forces [11]. Once flipped over, the SU-8 frame keeps the two CNT-electrodes from touching each other while containing the electrolyte within the cell.

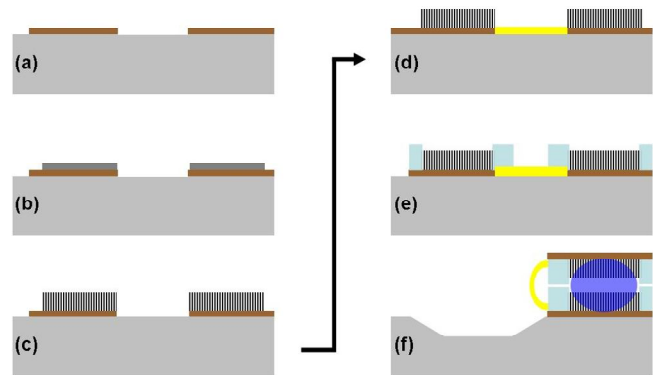


Fig. 2: Process flow for the CNT-origami electrochemical capacitor. (a) Deposit/pattern TiN layer. (b) Deposit/pattern catalyst layer. (c) Grow CNTs. (d) Deposit/pattern Au layer through lift-off. (e) Deposit/pattern SU-8 layer. (f) Release membrane, deposit electrolyte, and fold over flap.

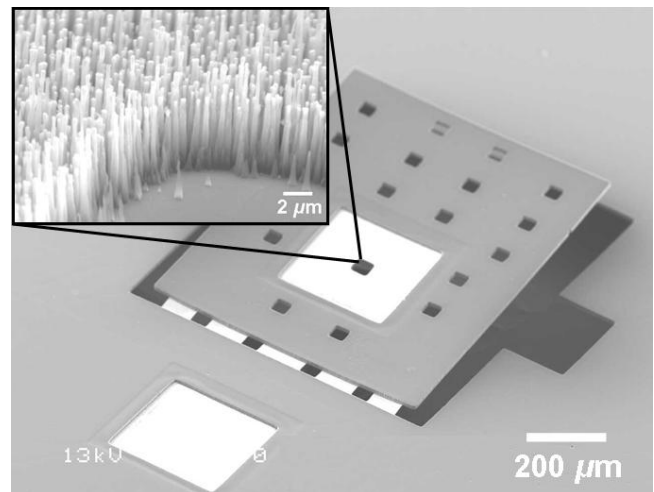
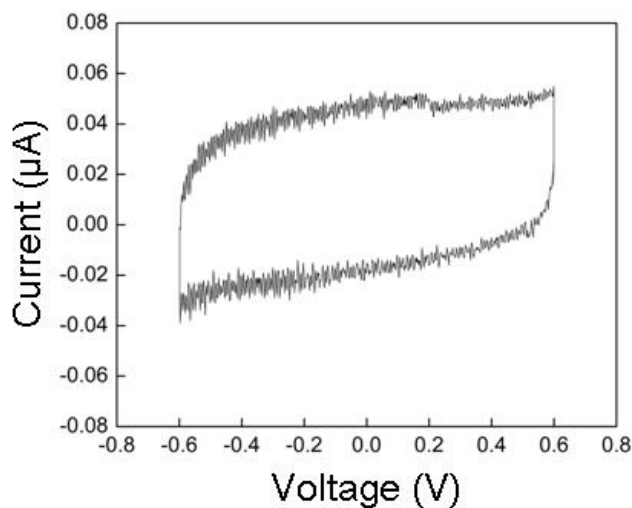


Fig. 3: SEM image of a CNT-origami supercapacitor prior to folding. The inset shows the CNT-covered electrode surface.

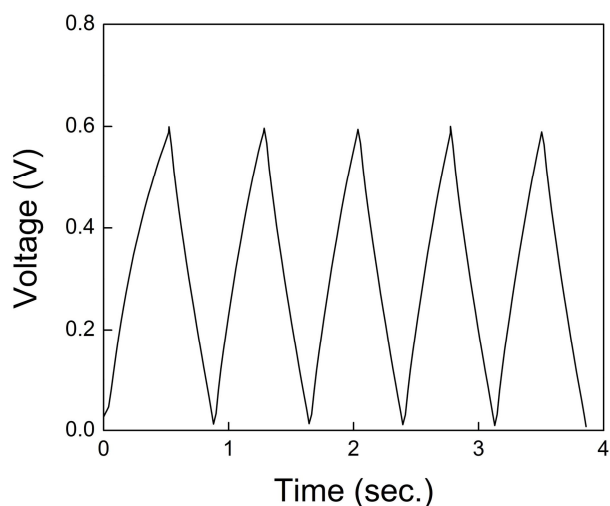
## TESTING AND RESULTS

After several electrochemical capacitors with MWCNT electrodes were successfully fabricated, their performance was characterized through cyclic voltammetry (CV), galvanostatic charge/discharge,

and electrical impedance spectroscopy (EIS). The electrochemical testing results are shown in Figures 4 and 5 for the two-electrode devices with a single electrode footprint of approximately  $6.25 \times 10^{-4} \text{ cm}^2$ . The two electrodes with the as-measured CNT geometry and density have a combined real surface area of approximately  $0.015 \text{ cm}^2$ . The CV curve was generated at a voltage scan rate of  $50 \text{ mV/s}$ , and the galvanostatic charge/discharge was done under a constant current of  $0.5 \mu\text{A}$ . The EIS was performed over a frequency range of  $5 \text{ MHz}$  to  $100 \text{ mHz}$  using a signal amplitude of  $10 \text{ mV}$ .



(a)



(b)

Fig. 4: (a) Cyclic voltammogram measured at a scan rate of  $50 \text{ mV/s}$ . (b) Galvanostatic charge/discharge profile recorded at  $\pm 0.5 \mu\text{A}$ .

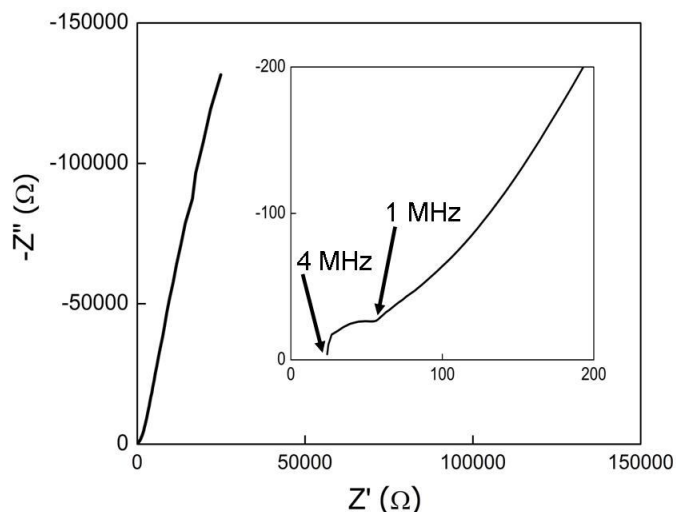


Fig. 5: Nyquist plot of the EIS results shown for frequencies between  $4 \text{ MHz}$  and  $4 \text{ Hz}$ .

Based on CV and galvanostatic charge-discharge measurements and using the equation  $C = I/(dV/dt)$ , a total system capacitance of approximately  $0.4 \mu\text{F}$  was obtained, which, given the slightly reduced electrode footprint of the new device, is comparable to the value of  $1.0 \mu\text{F}$  reported previously for the electrochemical capacitor based on Super P carbon black electrodes [4]. Different types of specific capacitances for both types of devices are summarized in Table 1. The CNT-based supercapacitor shows a slightly higher capacitance per surface area of electrode material since most of the CNT-electrode surface should be accessible for the ions; in the Super P device, some parts of the electrode surface is inaccessible due to the presence of small nanopores. For capacitance per volume and mass of electrode material, however, the CNT-based supercapacitor exhibits slightly lower values. This is most likely because only the outer most surfaces of the CNTs, which were quite thick with a less than optimal surface-area-to-volume ratio, contribute to charge storage.

The overall shape of the Nyquist plot shown in Fig. 5, which consists of a small semi-circle followed by a  $45^\circ$  Warburg impedance region at higher frequencies and a steep, almost vertical region at lower frequencies, is consistent with those found in literature for similar, albeit much larger, devices [14-16]. The Nyquist plot indicates an almost purely capacitive behavior at low frequencies and shows the frequency dependence of the ion diffusion and transport process at high frequencies. The equivalent series resistance (ESR), as determined from the  $Z'$ -intercept on the Nyquist plot, was approximately  $25 \Omega$ .

Table 1: Performance metrics for Super P and CNT-based electrochemical capacitors. All values shown are for the entire two-electrode system (\*Mass density of MWCNTs was taken to be  $0.6 \sim 2 \text{ g/cm}^3$  [12,13].)

Specific Capacitance	Super P	MWCNT
$\mu\text{F/cm}^2$ (on-chip area)	816	640
$\mu\text{F/cm}^2$ (theoretical surface area)	13	27
$\mu\text{F/cm}^3$ (theoretical volume)	$8.2 \times 10^{-4}$	$4.0 \times 10^{-4}$
F/g (theoretical mass)	4	$2 \sim 7^*$

## CONCLUSION

In conclusion, we have shown that a microscale electrochemical capacitor with vertically-aligned MWCNT electrodes can be made based on the origami process. The CNT-origami supercapacitor will be able to serve as an integrated, on-chip power source for various micro/nano-systems applications. We expect further performance improvements will result from optimizations of CNT geometry and density.

## ACKNOWLEDGMENTS

The authors would like to thank Professor Sang-Gook Kim and Dr. Hyung Woo Lee for valuable discussions and the Microsystems Technology Laboratories (MTL) staff for assistance with the fabrication. This research was funded by the Singapore-MIT Alliance for Research and Technology (SMART) Centre and the US Army Research Office (ARO) Institute for Soldier Nanotechnologies at MIT

## REFERENCES

[1] Conway B E 1999 *Electrochemical Supercapacitors: Scientific Fundamentals and Technological Applications* (New York, Plenum)

[2] Frackowiak E, Metenier K, Bertagna V, Beguin F 2000 Supercapacitor electrodes from multiwalled carbon nanotubes *Appl. Phys. Lett.* **77** 2421-2423

[3] Frackowiak E, Béguin F 2001 Carbon materials for the electrochemical storage of energy in capacitors *Carbon* **39** 937-950

[4] In H J, Kumar S, Shao-Horn Y, Barbastathis G

2006 Origami fabrication of nanostructured, three-dimensional devices: Electrochemical capacitors with carbon electrodes *Appl. Phys. Lett* **88** 083103-083105

[5] Zhang H, Cao G, Yang Y, Gu Z 2008 Comparison between electrochemical properties of aligned carbon nanotube array and entangled carbon nanotube electrodes *J. Electrochem. Soc.* **155** K19-K22

[6] Lu W, Qu L, Henry K, Dai L 2009 High performance electrochemical capacitors from aligned carbon nanotube electrodes and ionic liquid electrolytes *J. Power Sources* **189** 1270-1277

[7] An K H, *et al.* 2001 Supercapacitors using single-walled carbon nanotube electrodes *Adv. Mater.* **13** 497-500

[8] In H J, Lee H W, Kim S -G, Barbastathis G 2009 Nanomanufacturing of carbon nanotubes on titanium nitride *Int. J. Nanomanufacturing* (in press)

[9] Gao L, *et al.* 2008 Growth of aligned carbon nanotube arrays on metallic substrate and its application to supercapacitors *Sol. State Comm.* **146** 380-383

[10] Jiang Y Q, Zhou Q, Lin L Planar MEMS Supercapacitor using Carbon Nanotube Forests *IEEE MEMS 2009 (Sorrento, Italy, 25-29 January 2009)* 587-590

[11] Syms R R A, Yeatman E M, Bright V M, Whitesides G M 2003 Surface tension powered self-assembly of microstructures – The state-of-the-art *JMEMS* **12** 387-417

[12] Daniel S *et al.* 2006 A review of DNA functionalized/grafted carbon nanotubes and their characterization *Sens. Actuators. B* **122** 672-682.

[13] Kota A *et al.* 2007 Electrical and rheological percolation in polystyrene/MWCNT nanocomposite *Macromolecules* **40** 7400-7406.

[14] Wang Y, *et al.* 2009 Supercapacitor devices based on graphene materials *J. Phys. Chem. C* **113** 13103-13107

[15] Portet C, Taberna P L, Simon P, Laberty-Robert C 2004 Modification of Al current collector surface by sol-gel deposit for carbon-carbon supercapacitor applications *Electrochim. Acta* **49** 905-912

[16] Stoller M D, Park S, Zhu Y, An J, Ruoff R S 2008 Graphene-based supercapacitors *Nano Lett.* **8** 3498-3502